JACS
JOURNAL OF THE AMERICAN CHEMICAL SOCIETY

Article

pubs.acs.org/JACS

Preorganized Chromophores Facilitate Triplet Energy Migration, Annihilation and Upconverted Singlet Energy Collection

Prasenjit Mahato,[†] Nobuhiro Yanai,[*,†,‡] Melinda Sindoro,[§] Steve Granick,[§,⊥] and Nobuo Kimizuka[*,†]

[†]Department of Chemistry and Biochemistry, Graduate School of Engineering, Center for Molecular Systems (CMS), Kyushu University, 744 Moto-oka, Nishi-ku, Fukuoka 819-0395, Japan

[‡]PRESTO, JST, Honcho 4-1-8, Kawaguchi, Saitama 332-0012, Japan

[§]Department of Materials Science and Engineering, University of Illinois, Urbana, Illinois 61801, United States

[⊥]IBS Center for Soft and Living Matter, UNIST, Ulsan 689-798, South Korea

Supporting Information

ABSTRACT: Photon upconversion (UC) based on triplet−triplet annihilation (TTA) has the potential to enhance significantly photovoltaic and photocatalytic efficiencies by harnessing sub-bandgap photons, but the progress of this field is held back by the chemistry problem of how to preorganize multiple chromophores for efficient UC under weak solar irradiance. Recently, the first maximization of UC quantum yield at solar irradiance was achieved using fast triplet energy migration (TEM) in metal−organic frameworks (MOFs) with ordered acceptor arrays, but at the same time, a trade-off between fast TEM and high fluorescence efficiency was also found. Here, we provide a solution for this trade-off issue by developing a new strategy, triplet energy migration, annihilation and upconverted singlet energy collection (TEM−UPCON). The porous structure of acceptor-based MOF crystals allows triplet donor molecules to be accommodated without aggregation. The surface of donor-doped MOF nanocrystals is modified with highly fluorescent energy collectors through coordination bond formation. Thanks to the higher fluorescence quantum yield of surface-bound collectors than parent MOFs, the implementation of the energy collector greatly improves the total UC quantum yield. The UC quantum yield maximization behavior at ultralow excitation intensity was retained because the TTA events take place only in the MOF acceptors. The TEM−UPCON concept may be generalized to collectors with various functions and would lead to quantitative harvesting of upconverted energy, which is difficult to achieve in common molecular diffusion-based systems.

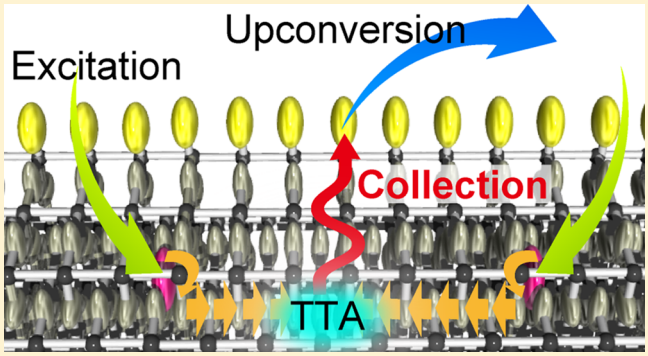

INTRODUCTION

Photon upconversion (UC) is a photophysical process where multiple photons are absorbed and their energies are combined to produce a photon of higher energy. Among the existing approaches, triplet−triplet annihilation (TTA)-based UC has attracted much attention because it operates with low-power noncoherent light like sunlight, thus holding enormous potential to enhance the efficiency of sunlight-powered energy production devices.[1−11] The mechanism of TTA-based UC is schematically shown in Figure S1, Supporting Information (SI). A donor molecule absorbs lower-energy photons and undergoes intersystem crossing (ISC) to the excited triplet state. This is followed by Dexter-type triplet−triplet energy transfer (TTET) with an acceptor, and a generated acceptor triplet in general has a long lifetime (~ms) because its transition to the singlet ground state is spin forbidden. The long lifetime of the triplet acceptors increases the opportunity to collide within their lifetimes and the resultant TTA generates a singlet excited state of the acceptor, thus giving rise to upconverted delayed fluorescence.

In spite of the expectations, it remains a challenge to achieve a high UC quantum yield at solar irradiance. Most of the previous examples of efficient UC used molecular diffusion in solvents and polymers for the TTET and TTA processes (Figure 1a).[2,12] However, the use of volatile solvents is not desirable for many applications, while molecular diffusion in solid polymer matrices is very limited. More fundamentally, the diffusion constant of chromophores in low-viscosity solvent, i.e., the rate constant of TTA, is not high enough to maximize the UC quantum yield at solar irradiance.[5]

It turns out that the key to resolve these basic problems is the chemistry to precisely control the arrangement of multiple chromophores. We have recently developed a triplet energy migration-based UC (TEM−UC) in molecular self-assembled

Received: February 20, 2016
Published: May 10, 2016

DOI: 10.1021/jacs.6b01652
J. Am. Chem. Soc. 2016, 138, 6541−6549

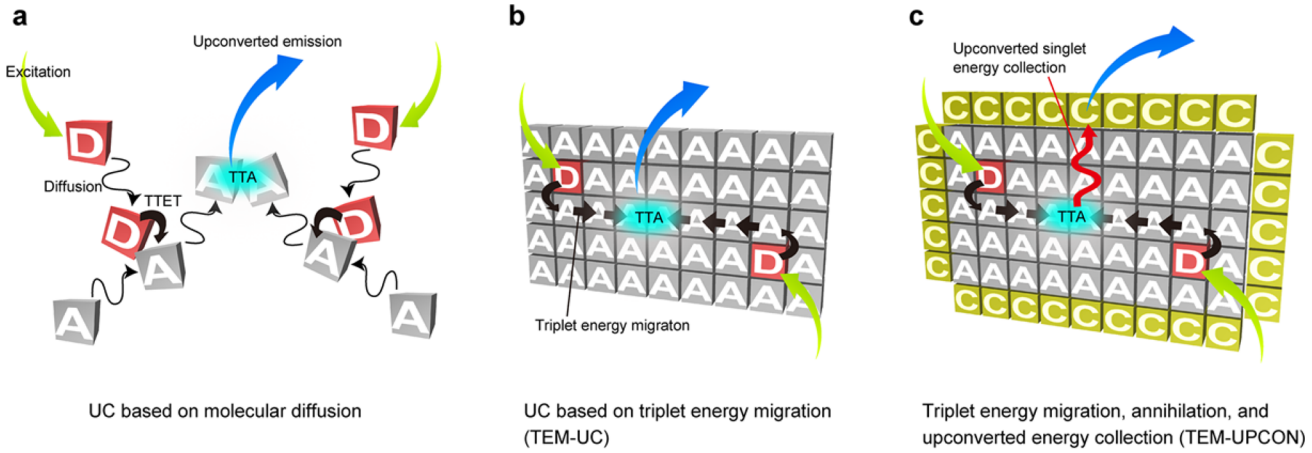

Figure 1. (a) Scheme for the UC mechanism based on molecular diffusion and collision. Red and gray boxes marked D and A represent triplet donor and acceptor molecules, respectively. Triplet state of donor, formed by intersystem crossing (ISC) from the photoexcited (green arrow) singlet state, diffuse and collide with acceptor, resulting in donor-to-acceptor triplet−triplet energy transfer (TTET). Two acceptor excited triplets again diffuse, collide, and annihilate to form a higher energy excited singlet, which consequently produces upconverted delayed fluorescence (blue arrow). (b) Scheme for the UC mechanism based on triplet energy migration (TEM). Excitation (green arrow) of donor molecules is followed by a sequence of TTET, TEM in the acceptor arrays, TTA between the excited acceptors, and higher energy UC emission (blue arrow). (c) Scheme for the UC mechanism based on triplet energy migration, annihilation, and upconverted singlet energy collection (TEM−UPCON). Yellow boxes marked C represent upconverted energy collector molecules. Similar to TEM−UC, the TTA takes place in the acceptor arrays. The resulting singlet energy migrates and reaches the energy collector that finally produces UC emission.

systems.[8−11,13−15] The molecular assembly directed TEM−UC enjoys fast triplet exciton diffusion in the aligned acceptor chromophores (Figure 1b). As a striking example, we have recently reported the first example of TEM−UC in metal−organic frameworks (MOFs) whose UC efficiency was maximized at solar irradiance for the first time by means of the surface-modification of MOF nanocrystals with donor chromophores and subsequent fast TEM in the MOFs.[11] Meanwhile, it remains difficult to ensure compatibility of the fast TEM with high photoluminescence efficiency. That is, TEM can be fast when neighboring acceptor molecules have close contact and large orbital overlap, while the acceptor fluorescence quantum yield often drops in such molecular arrays because of the prevailing nonradiative photorelaxation processes.

Here, we propose a fundamental solution to the trade-off issue that improves UC efficiency at solar irradiance by the following sequence of photophysical processes: triplet energy migration, annihilation and upconverted singlet energy collection (TEM−UPCON) to highly fluorescent moieties (Figure 1c). It creates a priority photoluminescence pathway that circumvents the nonradiative decay of the upconverted singlets, providing a means to overcome the trade-off issue. While the fluorescence resonance energy transfer (FRET) from upconverted excited singlet to other chromophores was utilized,[16−19]these examples were limited to in-solution molecular-diffusion-based systems, which severely limits their practical applications. In contrast, the current TEM−UPCON strategy has the important advantage of nonsolvent system. Furthermore, beyond the improvement of UC emission quantum yield, the TEM−UPCON concept may allow the direct energy harvesting to collectors with various functions. This not only circumvents the energy loss by absorption of upconverted photons by active materials, but also allows the quantitative harvesting of upconverted energy, both of which are difficult to achieve in the conventional molecular diffusion-based systems.

As a proof of concept, we modified the surface of an acceptor-based MOF with a highly fluorescent energy collector. To spatially separate the sensitization and photoluminescence events, the triplet donor and singlet energy collector are installed inside and outside the MOF crystal, respectively. Taking advantage of the porous structure of MOF, we could apply the so-called "bottle-around-ship" approach to incorporate a triplet donor Pt(II) octaethylporphyrin (PtOEP) inside the MOF without aggregation. This is in stark contrast to the case of dense molecular crystals, where the donor aggregation in acceptor crystals hampers the efficient triplet sensitization.[5,14,15,20] The PtOEP-doped MOF nanoparticles were synthesized and dispersed in a prototypical oxygen-barrier polymer, poly(vinyl alcohol) (PVOH). The obtained solid film showed a clear and stable upconverted emission in air, but its quantum yield was only 0.35% because of the low fluorescence quantum yield of the employed MOF. Remarkably, by modifying the donor-installed MOF nanoparticle surface with coumarin 343 fluorophore through coordination bond formation, the UC quantum yield was improved by a factor of 6.6 to 2.3%. Reflecting the original UC kinetics in the MOF structure, this saturated quantum yield was obtained from the very low excitation intensity, comparable to solar irradiance. The evaluation of UC data should include not only the saturated value of quantum yield, but also the excitation intensity to obtain that value. While the main purpose of this work is to propose the TEM−UPCON idea, the observed UC quantum yield is already comparable to that of state-of-the-art solid UC materials at low excitation intensity (~6 mW cm^{-2}).[11,21−23] The much improved UC efficiency at very low excitation intensity illustrates the promising potential of TEM−UPCON concept.

EXPERIMENTAL SECTION

Materials. All reagents and solvents were used as received unless otherwise noted. Pt(II) octaethylporphyrin (PtOEP) and poly(vinyl alcohol) (PVOH, M_w = 31 000−50 000 g mol^{-1}) were purchased from Sigma-Aldrich. A ligand 4,4′-(anthracene-9,10-diyl) dibenzoic acid

DOI: 10.1021/jacs.6b01652
J. Am. Chem. Soc. 2016, 138, 6541−6549

(adba) and a MOF $[Zn_2(adb)_2dabco]_n$ (adb =4,4′-(anthracene-9,10-diyl)dibenzoate, dabco =1,4-diazabicyclo[2.2.2]octane) were synthesized following the literature procedures.[24]

Bottle-around-Ship Synthesis of Donor@MOF. A mixture of adba (10 mg, 24 μmol), $Zn(NO_3)_2·6H_2O$ (7.1 mg, 24 μmol), dabco (1.34 mg, 12 μmol), PtOEP (1.7 mg, 2.4 μmol) and 1.3 mL *N*,*N*-dimethylformamide (DMF) were placed in a Teflon autoclave and heated at 120 °C for 48 h, then cooled to room temperature at 1 °C/min. Obtained light pink crystals (denoted as donor@MOF) were filtered through a 200 nm filter to remove small crystals, washed several times with DMF and dried at room temperature under vacuum. Yield = 11 mg (70%). Elemental analysis for $[Zn_2(C_{28}H_{16}O_4)_2(C_6H_{12}N_2)]·2.5DMF·5H_2O$. Calcd (%): C 61.9, H 5.34, N 4.67; found (%): C 61.9, H 5.29, N 4.62. Since the amount of donor included inside the MOF is small (ca. 0.1 mol %), its effect in the elemental analysis is negligible.

Bottle-around-Ship Synthesis of Donor@Nano-MOF. Donor-included MOF nanoparticles (denoted as donor@nano-MOF) were synthesized by using microwave instead of solvothermal method since it gives smaller crystal size probably due to faster nucleation by sudden increase of the reaction temperature. Microwave reactions were performed using the Biotage Initiator 2.5 under continuous stirring. A mixture of adba (2.5 mg; 6 μmol), $Zn(CH_3COO)_2·2H_2O$ (1.31 mg; 6 μmol), dabco (0.33 mg; 3 μmol), PtOEP (0.43 mg; 0.6 μmol), and 6 mL DMF was placed in a sealed glass vial and heated at 120 °C for 10 s in microwave. The power was around 31−33 W with temperature rise 3−4 °C/sec. It took 30−40 s to reach 120 °C and 14−15 min to cool down to room temperature. No pressure increase was observed during the synthesis. The sample was collected by centrifugation and washed several times with DMF, followed by drying in vacuum at room temperature. Yield = 0.4 mg (10%). This synthesis was repeated to obtain enough amount of material. Elemental analysis for $[Zn_2(C_{28}H_{16}O_4)_2(C_6H_{12}N_2)]·2DMF·2H_2O$. Calcd (%): C 64.92, H 4.97, N 4.45; found (%): C 65.0, H 4.99, N 4.48.

Surface Modification of the MOF Nanocrystals. The donor@nano-MOF nanocrystals (5 mg) were incubated in a DMF solution of Coumarin 343 (collector, 10 mM, 500 μL) at room temperature for 24 h, washed several times with DMF by centrifugation, and dried under vacuum at room temperature, giving collector-modified nanocrystals (denoted as donor@nano-MOF@collector).

Dispersing MOFs in PVOH Film. To *N*,*N*-dimethylacetamide (DMAc) solutions of PVOH (40 mg/mL), the donor@MOF, donor@nano-MOF, donor@nano-MOF@collector (10 wt % of PVOH) were dispersed, and dried on a quartz plate under vacuum at room temperature. All the characterizations of the composite films were carried out in the ambient condition without any sealing.

Measurements. Elemental analysis was conducted at the Elemental Analysis Center, Kyushu University. X-ray powder diffraction (XRPD) analysis was conducted on a BRUKER D2 PHASER with a Cu Kα source (λ = 1.5418 Å). Dynamic light scattering (DLS) measurements were performed on a Malvern Zeta-Sizer Nanoseries instrument. The samples were placed in small volume quartz cuvettes, and an average of 10 times of measurements was adopted. Transmission electron microscopy was conducted on a JEOL JEM-2010 with an acceleration voltage of 120 kV. UV−vis absorption spectra were recorded on a JASCO V-670 spectrophotometer at 25 °C. Quartz cell with 1 mm path length was used for solution samples. Fluorescence spectra were measured by using a PerkinElmer LS 55 spectrometer. Confocal laser scanning microscopy (CLSM) images were taken with a Carl Zeiss LSM510META apparatus equipped with a 40× objective. The excitation wavelength was chosen to be 405 nm. Time-resolved photoluminescence lifetime measurements were carried out by using time-correlated single photon counting lifetime spectroscopy system, HAMAMATSU Quantaurus-Tau C11367−02 (for prompt fluorescence lifetime)/C11567−01 (for phosphorescence and delayed fluorescence lifetime). The upconversion luminescence emission spectra were recorded on an Otsuka Electronics MCPD-7000 instrument with the excitation source of an external, adjustable 532 nm semiconductor laser. The UC quantum yields were determined by an absolute quantum yield measurement system using a laser excitation source and a calibrated spectrometer specially built by Hamamatsu Photonics.[9]

RESULTS AND DISCUSSION

Bottle-around-Ship Inclusion of Donor in MOF. It is appropriate to demonstrate the new strategy with well-known compositions. Therefore, we employed the benchmark composition in the UC research field; Pt(II) octaethylporphyrin (PtOEP) as donor and 9,10-diphenylanthracene (DPA) as acceptor. We employed MOFs constructed using the DPA-based ligand, 4,4′-(anthracene-9,10-diyl)dibenzoate (adb). The diffusion of triplet exciton in MOFs has been investigated recently,[11,25−27] and an adb-based MOF, $[Zn_2(adb)_2dabco]_n$ (adb = dabco = 1,4-diazabicyclo[2.2.2]octane)[24] was found to offer the particularly fast TEM thanks to the large orbital overlap between the DPA chromophores.[11] However, this MOF shows a low fluorescence efficiency, and thus we regard this MOF as a good example to demonstrate the TEM−UPCON strategy.

We have previously found that PtOEP is too large to be incorporated into the MOF nanopores.[11] We first incubated the MOF crystals in a DMF solution of PtOEP (5 mM) at room temperature for 72 h. The sample was filtered, washed several times with DMF, dried under vacuum at room temperature, and sealed in a quartz cell in an Ar-filled glovebox ($[O_2]$ < 0.1 ppm). Under excitation with a 532 nm laser (light intensity = 40 mW cm^{-2}), neither upconverted emission at 440 nm nor PtOEP phosphorescence at 645 nm were observed. This confirmed that PtOEP was not adsorbed into the MOF nanopores, which is reasonably understood by considering the large molecular size of PtOEP (1.5 nm × 1.5 nm × 0.66 nm) compared with the pore window of the employed MOF (0.73 nm × 0.46 nm).

Eddaoudi and co-workers have reported the encapsulation of catalytically active metalloporphyrins during the synthesis of MOFs.[28,29] We then applied this "bottle-around-ship" approach to incorporate the triplet donor in MOFs (Figure 2a). The MOF was synthesized in the presence of 0.1 mol equiv of PtOEP, and pale pink crystals were obtained (Figure 2c). The crystals were washed several times with DMF and dried in vacuum at room temperature. The phase purity of the obtained MOF crystals was confirmed by elemental analysis and by the good match between the X-ray powder diffraction (XRPD) pattern and the simulation pattern obtained from the crystal structure (Figure S2, SI). To determine the amount of PtOEP introduced into the MOF, we decomposed the MOF structure by treatment with the strong base tetrabutylammonium hydroxide (TBOH, 0.05 M) in DMF, and an absorption spectrum of the obtained solution was measured. From the Q-band absorbance of PtOEP at 535 nm, the donor-to-acceptor ratio was estimated as 1:1100. The donor-included MOF is denoted as donor@MOF.

Importantly, the donor was monomerically doped in MOF crystals, as confirmed by absorption and phosphorescence spectra. The absorption spectrum of PtOEP in MOF crystals did not show any shift compared with that in solution (Figure S3a, SI). The phosphorescence spectrum of PtOEP in MOF showed no peak at 780 nm originating from aggregated PtOEP species (Figure S3b, SI).[14,20] Considering that it is not easy to molecularly disperse donor molecules in dense acceptor molecular crystals,[5,14,15,20] the employment of porous MOF crystals is the powerful approach for aggregation-free donor doping.

DOI: 10.1021/jacs.6b01652
J. Am. Chem. Soc. 2016, 138, 6541−6549

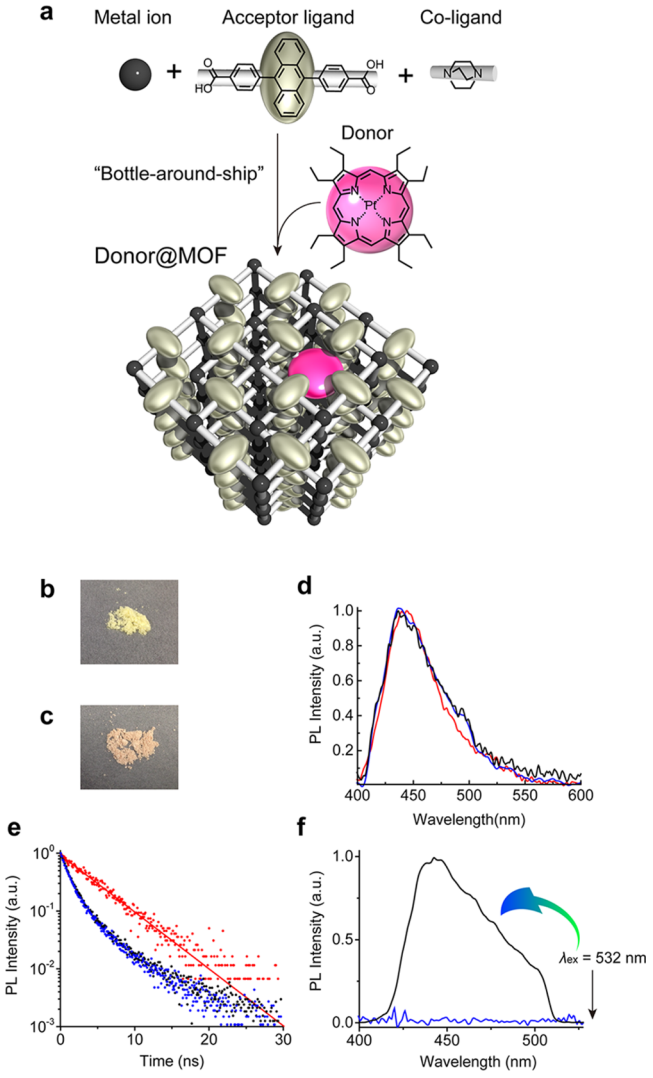

Figure 2. (a) Schematic representation of "bottle-around-ship" synthesis of donor@MOF. The MOF is constructed using acceptor-containing ligand, and the triplet donor PtOEP was introduced into the MOF structure during the crystallization process. Pictures of (b) the pristine MOF and (c) donor@MOF. (d) Fluorescence spectra of benzene solution of the ligand adba (red, 10 μM) and benzene dispersions (0.2 wt %) of the pristine MOF (blue) and donor@MOF (black) under excitation at λ_{ex} = 370 nm. (e) Fluorescence decays at 435 nm of the benzene solution of the ligand adba (red; 10 μM) and the benzene dispersions (0.2 wt %) of the pristine MOF (blue) and donor@MOF (black) under pulsed excitation at λ_{ex} = 365 nm. The adba solution followed the single exponential behavior with a lifetime of τ = 4.1 ns (red line). (f) Photoluminescence spectra of the donor@MOF (black, excitation light intensity = 15 mW cm^{-2}) and the MOF after being incubated in DMF solution of PtOEP, filtrated, washed, and dried in vacuum (blue, excitation light intensity = 200 mW cm^{-2}) under excitation of the 532 nm laser. The 532 nm notch filter and 510 nm short-pass filter were used to remove scattered incident light and donor phosphorescence. The samples were sealed in Ar atmosphere prior to the measurements.

The fluorescence property of MOF was intrinsically unaffected by the donor inclusion. Similar fluorescence spectra with an emission maximum at 440 nm were observed for the MOF crystals in the absence and presence of incorporated PtOEP (Figure 2d). The fluorescence lifetime measurement of the adba ligand in benzene solution showed a single exponential decay with a characteristic lifetime of τ = 4.1 ns (Figure 2e). Meanwhile, the MOF showed multicomponent fluorescence decay with a shorter average lifetime of 1.4 ns, which is a typical feature of condensed molecular systems. In MOF crystals, a singlet excited state formed by TTA also migrates over the frameworks, which would be easily trapped by defects and dissipated nonradiatively.[30] A detailed study of this aspect will be reported separately. It is to be noted that the MOFs with and without included PtOEP showed similar decay profiles, suggesting that the singlet−singlet back energy transfer from the acceptor ligand to the included donor is negligible because of the low content of the donor.

Interestingly, we observed an upconverted emission from the donor@MOF. For UC measurements, the crystalline powder of donor@MOF was placed between quartz plates and sealed in an Ar-filled glovebox. Upon excitation with a green laser (λ_{ex} = 532 nm), a strong upconverted emission around 440 nm was observed (Figure 2f). The observed UC emission clearly indicates the successful inclusion of PtOEP inside the MOF frameworks, because no UC emission was obtained for the MOF crystals that were incubated in PtOEP solution to absorb physically the donor on the surface and washed with DMF (Figure 2f). Moreover, when the bottle-around-ship method of donor inclusion was similarly applied to the nonporous adb-based MOF $[Zn(adb)\ (DEF)_2]_n$ (DEF = *N*,*N*-diethylformamide),[11] neither upconverted emission nor PtOEP phosphorescence were observed. These control experiments clearly indicate that the porous structure is a prerequisite for the bottle-around-ship inclusion of triplet donor. Upon excitation by the 532 nm laser, an excited triplet state of PtOEP is generated, and this transfers the triplet energy to the surrounding adb ligands of the MOF. The sensitized triplet energy further migrates through the acceptor arrays and undergoes collision with another acceptor triplet to generate the higher-energy excited singlet state by TTA, which consequently produces upconverted blue emission. As the UC emission intensity of the neat donor@MOF crystals was not perfectly stable, especially at high-power excitation, we embedded this UC material into a polymeric matrix and quantitatively scrutinized their UC properties, as discussed below.

Air-Stable TEM−UC Emission in an Oxygen-Barrier Matrix. One of the important advantages of self-assembly based UC is that it allows immobilization of TEM systems in any solid matrix. The UC emission is sensitive to air because the triplet excited state is readily quenched by molecular oxygen. It is possible to avoid this oxygen quenching by using polymer matrices with excellent oxygen-barrier properties.[31,32] The necessary characteristics of a barrier polymer include a high interchain cohesive energy density (high polarity), high glass transition temperature, and low free volume.[33] The higher a polymer's cohesive energy density, the more difficult it is for the polymer chains to form voids that allow oxygen to pass.[33] The glass transition temperature should be much higher than room temperature to reduce polymer mobility. The reduction of free volume leads to a decrease in gas mobility in the glassy polymer.[34] We worked with the prototypical oxygen-barrier polymer, poly(vinyl alcohol) (PVOH). PVOH and its copolymers are commonly used in the packaging and food industries to protect contents from exposure to oxygen molecules. The high transparency and film-forming properties of PVOH are also suitable for making optically active materials.

DOI: 10.1021/jacs.6b01652
J. Am. Chem. Soc. 2016, 138, 6541−6549

In general, the light scattering from polycrystalline materials can be a critical issue for making optically active films. As reported previously,[11] this problem can be avoided by downsizing the crystals to a nanoscale. By employing $Zn(CH_3COO)_2{\cdot}2H_2O$ as the metal source and short-time microwave heating, monodisperse MOF nanoparticles (nano-MOF) were obtained. It indicates that the use of acetate salt and rapid microwave heating have contributed to accelerating the nucleation process, which is essential to prepare nano-MOFs.[35,36] The synthesized nano-MOF was characterized by elemental analysis, dynamic light scattering (DLS) measurements for DMF dispersions (an average particle size; 140 nm, Figure 3a), transmission electron microscopy (crystal size ~120 nm, Figure 3b) and XRPD measurement (Figure S4, SI). Similar to the case of large MOF crystals, the bottle-around-ship method allowed 0.1 mol % of the donor PtOEP to be successfully incorporated in the MOF nanoparticles during the crystallization process. The obtained sample is called donor@nano-MOF.

Transparent films were prepared using the nanosized crystals (Figure S5, SI). The donor@nano-MOF sample was dispersed in *N*,*N*-dimethylacetamide (DMAc) solution of PVOH (donor@nano-MOF is 10 wt % of PVOH), and the dispersion was cast on a quartz plate and dried in vacuum at room temperature. Remarkably, even in the open air, the obtained film showed a stable upconverted blue emission at around 440 nm upon exposure to the 532 nm green laser (Figure 3c). The stability of the UC emission was confirmed by time-dependent UC emission measurement of the composite film in the open air. The UC emission intensity did not show any change for 40 min upon continuous exposure to the 532 nm laser with a light intensity of 65 mW cm^{-2} (Figure 3d). This demonstrates the undisturbed operation of TTA-based UC in air.

The time-resolved photoluminescence at 440 nm under 532 nm pulsed excitation showed a ms-scale decay (Figure 3e). We found no rise in the examined time scale, reflecting the fast donor-to-acceptor triplet−triplet energy transfer. When both linear and nonlinear decay pathways are simultaneously present as in UC emission by TTA, the UC emission decay obeys to

$$I_{UC}(t) \propto [T_A^2]_t = [T_A^2]_0 \left(\frac{1 - \Phi_{TTA}}{\exp[k_A t] - \Phi_{TTA}} \right)^2 \quad (1)$$

where T_A is the population density of acceptor triplet, Φ_{TTA} is TTA quantum yield, and k_A is the acceptor natural decay rate ($k_A = \tau_T^{-1}$, τ_T: acceptor triplet lifetime).[22,30,37] The fitting result gave a quantitative TTA quantum yield $\Phi_{TTA} = 0.97$ and a ms-scale lifetime $\tau_T = 3.5$ ms, confirming the efficient TTA-based UC process.

The efficiency of donor-to-acceptor TTET was evaluated by measuring the phosphorescence lifetime of donor PtOEP. The phosphorescence decay at 645 nm of PtOEP dispersed in PVOH showed a single exponential decay with a lifetime of $\tau_0 = 93$ μs (Figure S6, SI). Inside the nano-MOF crystals, the phosphorescence lifetime decreased to $\tau = 61$ μs. The TTET efficiency was determined to be $\Phi_{ET} = 1 - \tau/\tau_0 = 34\%$. We have reported that when crystals of pristine MOF (0.2 wt %) were dispersed in a benzene solution of PtOEP (30 μM), the TTET efficiency was only 7%.[11] The TTET process takes place via the electron-exchange Dexter mechanism, and it requires close contact of donor and acceptor molecules within ca. 1 nm to have effective orbital overlap between them.[38] Inside the MOF, the donor molecules are surrounded by triplet acceptor struts in close proximity. This produced a 5-fold increment of TTET efficiency compared with the solution dispersion system, where donor molecules need to diffuse to the MOF surface during their lifetime. The optimization of donor and MOF structures may further increase the TTET efficiency.

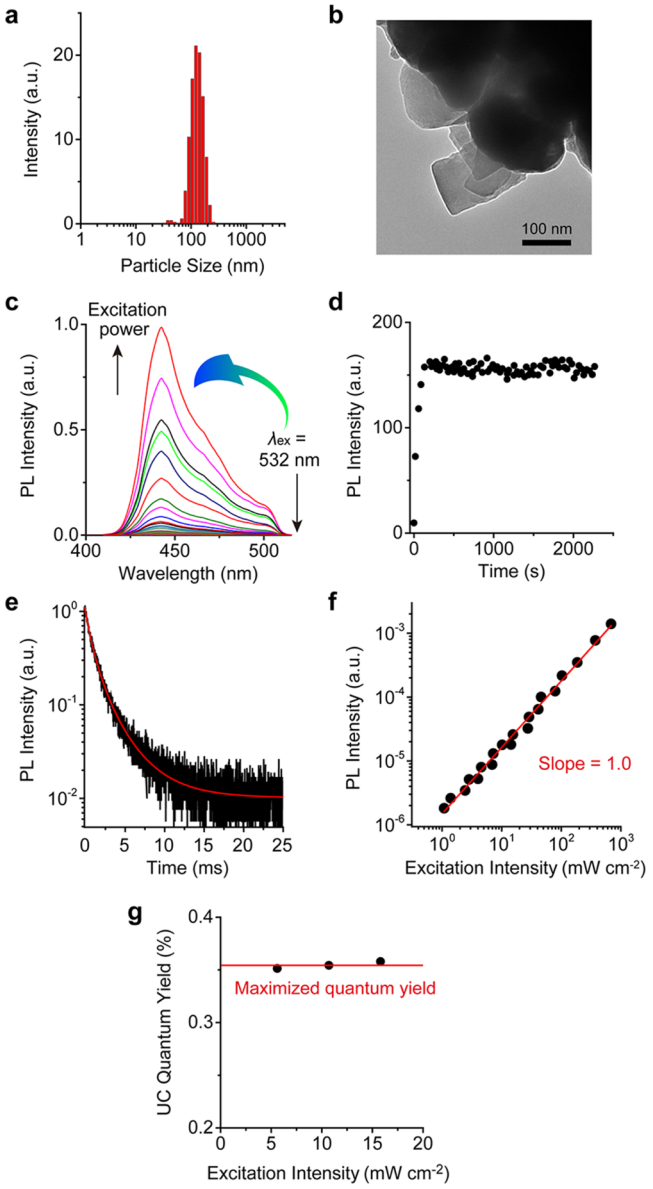

Figure 3. (a) Particle size distribution obtained by DLS measurements of nano-MOF dispersed in DMF. (b) Typical transmission electron microscopy image of nano-MOF crystals attached at the edge of copper grid. (c) In-air photoluminescence spectra of donor@nano-MOF in PVOH film at different incident light intensity of 532 nm laser. The 532 nm notch filter and 510 nm short-pass filter were used to remove scattered incident light. (d) Time dependence of in-air UC emission intensity of the donor@nano-MOF in PVOH film at 450 nm upon continuous excitation at 532 nm with a laser light intensity of 65 mW cm^{-2}. (e) In-air photoluminescence decay at 445 nm of the donor@nano-MOF in PVOH film under pulsed excitation at 532 nm. Fitting result using eq 1 is shown as red line. (f) UC emission intensity for the donor@nano-MOF in PVOH film as a function of the excitation intensity in air ($\lambda_{ex} = 532$ nm). The linear fit with a slope of 1.0 is shown. (g) In-air UC quantum yield Φ_{UC} of the donor@nano-MOF in PVOH film with different incident light intensity of 532 nm laser.

DOI: 10.1021/jacs.6b01652
J. Am. Chem. Soc. 2016, 138, 6541−6549

As discussed in our previous work,[11] the quantitative TTA process from low excitation intensity was confirmed from consideration of the figure-of-merit parameter, the threshold excitation intensity (I_{th}),[39] characterizing UC systems. The I_{th} is the transition excitation intensity from quadratic to linear excitation intensity dependence, and it defines the useful irradiance working range.[37,39,40] It has been reported that I_{th} follows the relationship[39]

$$I_{th} = (\alpha \Phi_{ET} 8\pi D_T a_0)^{-1} (\tau_T)^{-2} \quad (2)$$

where α is the absorption coefficient at the excitation wavelength (2.9 cm^{-1}), Φ_{ET} is the donor-to-acceptor TTET efficiency (34%), D_T is the diffusion constant of the acceptor triplet (2.4×10^{-3} cm^2 s^{-1} for the employed MOF), a_0 is the annihilation distance between acceptor triplets (9.1 Å for DPA triplets[39]) and τ_T is the lifetime of the acceptor triplet (3.5 ms). From these parameters, we estimated a notably low I_{th} of 0.0057 mW cm^{-2}, which is more than 200 times smaller than the solar irradiance at the excitation wavelength (1.6 mW cm^{-2} at 532 ± 5 nm). Such a low I_{th} value is fully consistent with the observed linear excitation intensity dependence from as low as 1 mW cm^{-2} (Figure 3f).

As expected from the ultralow I_{th} value, the in-air UC quantum yield Φ_{UC} of the composite film was maximized from very low excitation intensity. The Φ_{UC} value was measured using an integrating sphere and the 532 nm laser as excitation source.[9] Note that the TTA-based UC process uses two photons to produce one photon, and therefore the theoretical maximum of Φ_{UC} should be set as 50%.[5,41,42] Remarkably, even under exposure to air, the Φ_{UC} of the composite film was maximized from a low laser light intensity around 6 mW cm^{-2} (Figure 3g). The Φ_{UC} value remained constant with further increase in the excitation intensity, confirming the quantitative TTA process along with the low I_{th} value. We note that even free molecular diffusion in low-viscosity solvent cannot achieve the Φ_{UC} maximization at the solar irradiance because of the diffusion limit of molecules,[5] demonstrating the importance of TEM–UC.

The maximized Φ_{UC} value was 0.35%, which is not high even for solid-state upconverter. To understand this, we checked the related parameters. The Φ_{UC} is described by the following equation[5]

$$\Phi_{UC} = \frac{1}{2} f \Phi_{ISC} \Phi_{ET} \Phi_{TTA} \Phi_{FL} \quad (3)$$

where Φ_{ISC}, Φ_{ET}, Φ_{TTA}, and Φ_{FL} represent the quantum efficiencies of donor ISC, donor-to-acceptor TTET, acceptor–acceptor TTA and acceptor fluorescence, and f is the statistical probability for obtaining a singlet excited state after the annihilation of two triplet states. In the current system, Φ_{ISC} is known to be 1, and Φ_{ET} was estimated as 0.32. In the saturation regime, where Φ_{UC} is a maximum and constant, the Φ_{TTA} can be assumed to be 1.[5] Note that Φ_{TTA} represents the ratio of acceptor T_1 used for TTA among all sensitized T_1, not the efficiency of S_1 formation by TTA (that is expressed as f). It is common that Φ_{TTA} is 1 in the saturated regime and f is below 1 depending on the energy levels of T_n ($n \geq 2$) that can be the deactivation channel. The Φ_{FL} was experimentally determined as 6.5% by measuring the absolute quantum yield in the integrating sphere. The f value is thus calculated as 0.34. The obtained f value is close to the reported value for DPA in solution (0.4–0.5),[5,42] supporting the validity of the results. This consideration suggests that the improvement of MOF fluorescence quantum yield Φ_{FL} (6.5%) is the key to achieving higher total UC efficiency.

Upconverted Energy Collection at the Nano-MOF Crystal Surface. We demonstrate that the major issue of the MOF-based TEM–UC system, that is, the UC quantum yield being low, can be fundamentally overcome by upconverted singlet energy collection (UPCON) to highly fluorescent molecules (Figure 4a). We chose coumarin 343 as an energy collector. The absorption band of coumarin 343 covers the

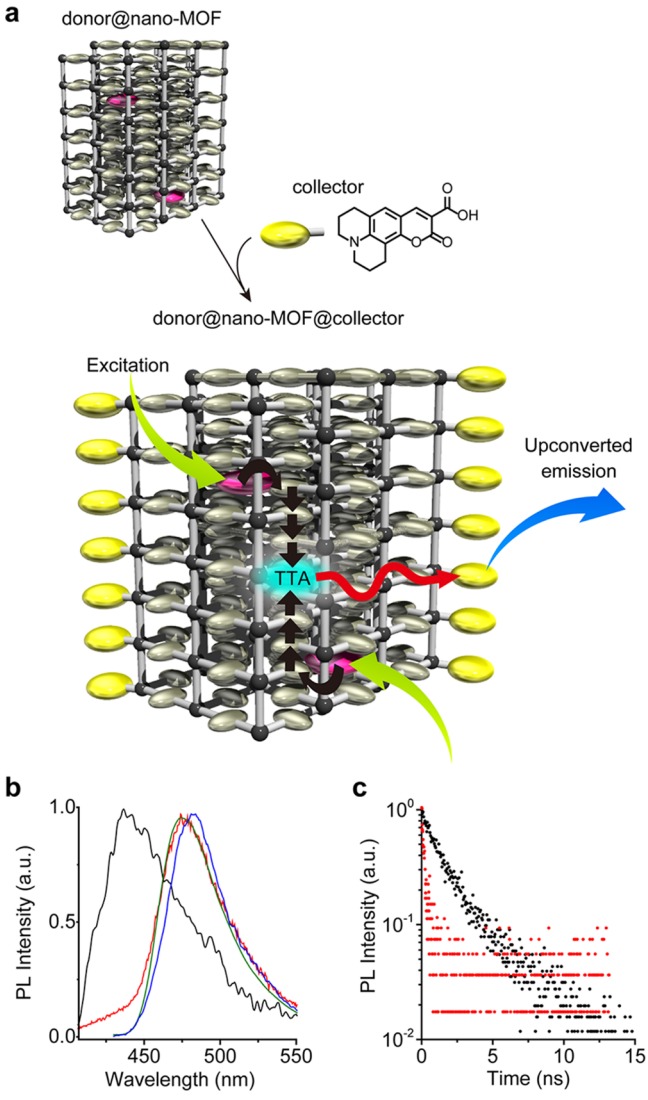

Figure 4. (a) Schematic representation of TEM–UPCON system. The surface of nano-MOF crystals is modified with a carboxylate-containing energy collector (coumarin 343). Excitation (green arrow) of donor molecules is followed by a sequence of TTET to the surrounding acceptor struts of MOF, TEM in the acceptor arrays, TTA between the excited acceptors, upconverted singlet energy migration and harvesting by the collector molecules and finally higher energy UC emission (blue arrow). (b) Fluorescence spectra of benzene dispersions (0.2 wt %) of nano-MOF (black) and donor@nano-MOF@collector (red) under excitation at λ_{ex} = 370 nm, and fluorescence spectra of methanol solution of coumarin 343 (10 μM) in the absence (blue) and presence (green) of 200 μM NaOH under excitation at λ_{ex} = 420 nm. (c) Fluorescence decays at 415 nm of benzene dispersions (0.2 wt %) of nano-MOF (black) and donor@nano-MOF@collector (red) under pulsed excitation at λ_{ex} = 365 nm.

DOI: 10.1021/jacs.6b01652
J. Am. Chem. Soc. 2016, 138, 6541–6549

emission range of the MOF (Figure S7, SI). Various modification methods of MOF exterior surface have been developed recently.[36,43−50] In particular, it has been reported that the surface carboxylate ligands of MOF crystals can be easily exchanged with fluorescent dyes having carboxylate groups.[45,47] Coumarin 343 has a carboxylate group that is expected to bind to the MOF crystal surface. To confirm this surface modification, large micrometre-sized MOF crystals were incubated in DMF solution of coumarin 343, washed with DMF, and observed under a confocal laser scanning microscope (CLSM). A bright coumarin emission at around 470 nm was selectively observed at the crystal surface (Figure S8, SI). In addition, a control experiment was carried out using coumarin 153, which does not have a carboxylate group. After incubating MOF nanoparticles in the DMF solution of coumarin 153 at room temperature for 24 h and subsequently washing with DMF several times, no fluorescence of coumarin 153 was observed. This result clearly indicates that the coumarin 343 molecules bind to the MOF crystal surfaces by forming coordination bonds between their carboxylate groups and surface Zn ions.[45]

The surface-modified coumarin 343 molecules could effectively collect the singlet excited energy from donor@nano-MOF. The donor@nano-MOF particles were modified with coumarin 343, and the obtained sample is called donor@nano-MOF@collector. In the photoluminescence spectrum of donor@nano-MOF@collector under excitation at 370 nm, the fluorescence from nano-MOF at 445 nm almost disappeared, and the coumarin 343 emission at 475 nm emerged (Figure 4b). Note that the fluorescence peak at 475 nm of donor@nano-MOF@collector nicely matches the peak of deprotonated coumarin 343 in basic solution, but it is different from the fluorescence band at 482 nm of neutral coumarin 343 (Figure 4b). This confirms that the nano-MOF surface is modified with deprotonated coumarin 343 molecules through the formation of coordination bond. The fluorescence lifetime of nano-MOF became much shorter by the collector modification (Figure 4c). These results prove that the absorbed photon energy was successfully harvested by the singlet energy migration among the MOF ligand arrays and subsequent fluorescence resonance energy transfer (FRET) to the surface collector molecules. While it was difficult to estimate precisely the amount of surface coumarin after decomposing the MOF structure because it is too small to detect by ^{1}H NMR and the absorption of coumarin 343 overlaps with that of the acceptor ligand, the surface coverage of coumarin was sufficient to harvest most of the singlet excited energy from the nano-MOF. Remarkably, the absolute fluorescence quantum yield (λ_{ex} = 370 nm) was successfully improved from 6.5% (donor@nano-MOF) to 40% (donor@nano-MOF@collector) by surface modification with the coumarin energy collector.

The UPCON approach using the coumarin energy collector allowed us to improve significantly the total UC quantum yield. A transparent film of donor@nano-MOF@collector particles (10 wt %) in PVOH was fabricated by drying a DMAc solution of PVOH and nanoparticles under vacuum at room temperature (Figure 5a). The yellow color comes from the surface coumarin dyes. The donor phosphorescence lifetime measurements showed that the donor-to-acceptor TTET efficiency in the solid film was estimated as Φ_{ET} = 34%, which is similar to the Φ_{ET} value of the PVOH film containing donor@nano-MOF particles (Figure S9a, SI). Upon excitation with the 532 nm green laser, a bright cyan emission at 475 nm was observed

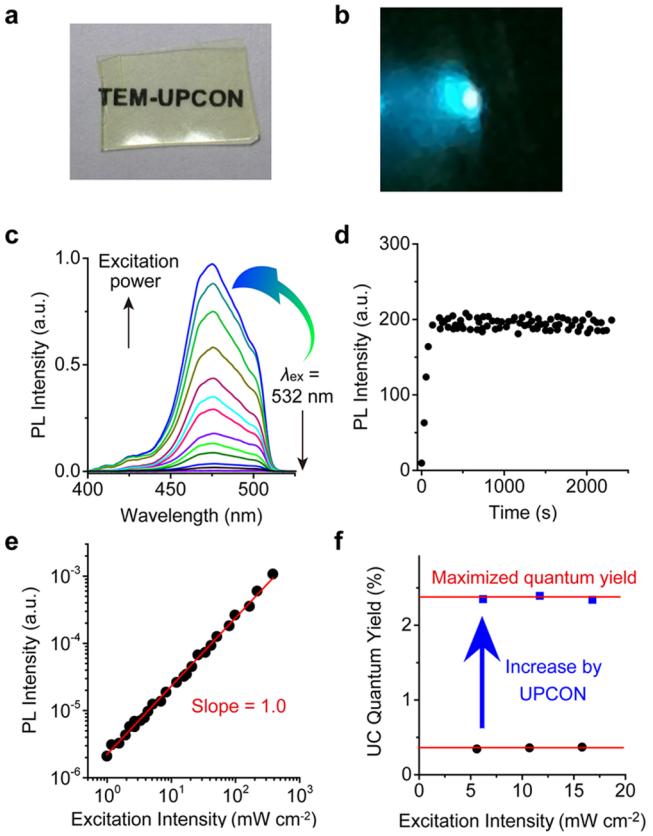

Figure 5. Picture of donor@nano-MOF@collector in PVOH film under (a) white light and (b) 532 nm laser excitation (532 nm notch filter and 510 nm short pass filter were used to remove scattered laser light and residual donor phosphorescence). (c) In-air photoluminescence spectra of donor@nano-MOF@collector in PVOH film at different incident light intensity of 532 nm laser. The 532 nm notch filter and 510 nm short-pass filter were used to remove scattered incident light and residual donor phosphorescence. (d) Time dependence of in-air UC emission intensity of donor@nano-MOF@collector in PVOH film at 475 nm upon continuous excitation at 532 nm with a laser light intensity of 35 mW cm^{-2}. (e) UC emission intensity for the donor@nano-MOF@collector in PVOH film as a function of the excitation intensity in air (λ_{ex} = 532 nm). The linear fit with a slope 1.0 is shown. (f) In-air UC quantum yield Φ_{UC} of donor@nano-MOF (circles) and donor@nano-MOF@collector (squares) in PVOH film with different incident light intensity of 532 nm laser.

from the PVOH film of donor@nano-MOF@collector in air (Figure 5b, c). The spectral shape of this UC emission shows a good match with the deprotonated coumarin 343 fluorescence (Figure 4b). We note that neither the coumarin by itself nor a mixed solution of coumarin and PtOEP showed any UC emission (Figure S10, SI). This proves that the coumarin only harvests upconverted singlet energy and does not accept triplet energy because of its high triplet energy level at 2.2 eV.[51] A ms-scale decay of the UC emission also confirms its mechanism mediated by a long-lived triplet state. Interestingly, the triplet lifetime of donor@nano-MOF@collector (τ_T = 3.3 ms) was identical to that of donor@nano-MOF (τ_T = 3.5 ms), which clearly indicates that the UC emission dynamics of coumarin collector at donor@nano-MOF surface simply follows the one of parent donor@nano-MOF (Figure S9b, SI). This is reasonable from the kinetics of singlet exciton transfer from nano-MOF to coumarin collector (Figure S11, SI). Unlike the nano-MOF fluorescence, the coumarin fluorescence showed

DOI: 10.1021/jacs.6b01652
J. Am. Chem. Soc. 2016, 138, 6541−6549

the rise within 1 ns, reflecting the singlet energy collection process. Although this energy collection process is too fast to further analyze using our setup, the singlet energy collection takes place in the nanosecond scale. Therefore, it has almost no influence on the millisecond-scale UC emission kinetics. Similar to the case of donor@nano-MOF, the observed UC emission is stable under continuous excitation for 40 min under ambient atmosphere (Figure 5d, laser intensity = 35 mW cm^{-2}). A linear excitation intensity dependence of the UC emission intensity was observed from the very low excitation intensity for the donor@nano-MOF@collectorPVOH film (Figure 5e).

According to the Lambert−Beer law, the light penetration depth of donor@nano-MOF@collector in PVOH film is $D_{exc} = 1/\alpha = 0.34$ cm. This is much larger than the dimension of nano-MOF, and thus the excitation should occur throughout the crystallites. The triplet diffusion length can be estimated as $L_T = (D_T\tau_T)^{1/2} = 28$ μm, which is much larger than the nano-MOF crystal dimension. Therefore, once PtOEP triplets are generated by the incident light, they transfer the triplet energy to the nearby acceptor strut of the MOF, and the produced triplet excitons migrate all over the MOF nanocrystals. In addition, thanks to the small nanosized dimension of MOF crystals, the singlet energy formed by TTA is almost quantitatively collected by the surface coumarin molecules.

Significantly, the UC quantum yield was maximized at 2.3% from the very low excitation intensity of 6.2 mW cm^{-2} (Figure 5f). Reflecting the improved fluorescence quantum yield, the obtained UC quantum yield becomes 6.6 times higher than the donor@nano-MOF film. The total UC quantum yield would be further improved by tuning the donor and collector structure to enhance the TTET and fluorescence efficiencies. The UPCON strategy solves the intrinsic trade-off problem of TEM−UC by improving the UC quantum yield while maintaining the maximization behavior of UC quantum yield from ultralow excitation intensity.

CONCLUSIONS

In conclusion, this work provides an essential solution for overcoming the challenge of TEM−UC, namely maximum and improved UC quantum yield at weak solar irradiance, by developing a new triplet energy migration, annihilation and subsequent upconverted singlet energy collection (TEM−UPCON) strategy. The precise preorganization of multiple chromophores is found to be the key to achieve efficient TEM−UPCON systems. First, the acceptor molecules are regularly and densely aligned, and donor molecules are accommodated in the acceptor crystalline lattice without aggregation. The donor molecules usually tend to aggregate in dense acceptor molecular crystals, but the porous structure of MOF crystals allowed the aggregation-free donor accommodation via the bottle-around-ship route. Second, this hybrid crystal is downsized to nanoscale in order to reduce the light scattering. This was achieved by controlling the MOF crystallization process. Third, the surface of the nanocrystals is modified with singlet energy collector with high fluorescence quantum yield. The collector coumarin molecules were successfully attached to the MOF nanocrystal surface through the formation of noncovalent coordination bonds.

Toward the true chemistry innovation based on UC, composition and organization are the two wheels of a cart. This work offers the important contribution to the latter. The natural next step is the generalization of the current TEM−UPCON concept to other donor−acceptor−collector compositions. Particularly, NIR-to-visible UC is expected for its application to photovoltaic devices,[7] and visible-to-UV UC for photocatalytic reactions.[52]

In a rational extension of the TEM−UPCON concept, instead of giving UC emission, the upconverted singlet energy can be directly collected by functional materials. The generalization of singlet energy collectors to photocatalytic, photovoltaic, sensing, sensitizing (ex. photodynamic therapy) and active (ex. drug)-releasing materials may bring exciting functions workable under extremely weak light irradiation.[53]

ASSOCIATED CONTENT

Supporting Information

The Supporting Information is available free of charge on the ACS Publications website at DOI: 10.1021/jacs.6b01652.

A scheme of TTA-based UC mechanism, XRPD patterns, absorption and photoluminescence spectra, picture of solid film, photoluminescence decays, CLSM images. (PDF)

AUTHOR INFORMATION

Corresponding Authors

*yanai@mail.cstm.kyushu-u.ac.jp

*n-kimi@mail.cstm.kyushu-u.ac.jp

Notes

The authors declare no competing financial interest.

ACKNOWLEDGMENTS

This work was partly supported by the JSPS-NSF International Collaborations in Chemistry (ICC) program, a Grants-in-Aid for Scientific Research (S) (25220805), a Grants-in-Aid for Young Scientists (B) (26810036), a Grant-in-Aid for Scientific Research on Innovative Area (16H00844) from the Ministry of Education, Culture Sports, Science and Technology of Japan, and the Asahi Glass Foundation. M.S. was supported by the National Science Foundation, Grant NSF CHE 13-03757. S.G. acknowledges support from the Institute for Basic Science, Project Code IBS-R020-D1.

REFERENCES

(1) Baluschev, S.; Miteva, T.; Yakutkin, V.; Nelles, G.; Yasuda, A.; Wegner, G. *Phys. Rev. Lett.* **2006**, *97*, 143903.

(2) Singh-Rachford, T. N.; Castellano, F. N. *Coord. Chem. Rev.* **2010**, *254*, 2560.

(3) Zhao, J. Z.; Ji, S. M.; Guo, H. M. *RSC Adv.* **2011**, *1*, 937.

(4) Kim, J. H.; Kim, J. H. *J. Am. Chem. Soc.* **2012**, *134*, 17478.

(5) Monguzzi, A.; Tubino, R.; Hoseinkhani, S.; Campione, M.; Meinardi, F. *Phys. Chem. Chem. Phys.* **2012**, *14*, 4322.

(6) Simon, Y. C.; Weder, C. *J. Mater. Chem.* **2012**, *22*, 20817.

(7) Schulze, T. F.; Schmidt, T. W. *Energy Environ. Sci.* **2015**, *8*, 103.

(8) Duan, P.; Yanai, N.; Kimizuka, N. *J. Am. Chem. Soc.* **2013**, *135*, 19056.

(9) Duan, P.; Yanai, N.; Nagatomi, H.; Kimizuka, N. *J. Am. Chem. Soc.* **2015**, *137*, 1887.

(10) Ogawa, T.; Yanai, N.; Monguzzi, A.; Kimizuka, N. *Sci. Rep.* **2015**, *5*, 10882.

(11) Mahato, P.; Monguzzi, A.; Yanai, N.; Yamada, T.; Kimizuka, N. *Nat. Mater.* **2015**, *14*, 924.

(12) Zhou, J.; Liu, Q.; Feng, W.; Sun, Y.; Li, F. Y. *Chem. Rev.* **2015**, *115*, 395.

(13) Baluschev, S.; Yakutkin, V.; Wegner, G.; Minch, B.; Miteva, T.; Nelles, G.; Yasuda, A. *J. Appl. Phys.* **2007**, *101*, 023101.

(14) Vadrucci, R.; Weder, C.; Simon, Y. C. *J. Mater. Chem. C* **2014**, *2*, 2837.

DOI: 10.1021/jacs.6b01652
J. Am. Chem. Soc. 2016, 138, 6541−6549

(15) Hosoyamada, M.; Yanai, N.; Ogawa, T.; Kimizuka, N. *Chem. - Eur. J.* **2016**, *22*, 2060.
(16) Kim, J. H.; Deng, F.; Castellano, F. N.; Kim, J. H. *ACS Photonics* **2014**, *1*, 382.
(17) Wang, W. P.; Liu, Q.; Zhan, C. Y.; Barhoumi, A.; Yang, T. S.; Wylie, R. G.; Armstrong, P. A.; Kohane, D. S. *Nano Lett.* **2015**, *15*, 6332.
(18) Xu, K. J.; Zhao, J. Z.; Cui, X. N.; Ma, J. *Chem. Commun.* **2015**, *51*, 1803.
(19) Askes, S. H. C.; Kloz, M.; Bruylants, G.; Kennis, J. T. M.; Bonnet, S. *Phys. Chem. Chem. Phys.* **2015**, *17*, 27380.
(20) Goudarzi, H.; Keivanidis, P. E. *J. Phys. Chem. C* **2014**, *118*, 14256.
(21) Kim, J. H.; Deng, F.; Castellano, F. N.; Kim, J. H. *Chem. Mater.* **2012**, *24*, 2250.
(22) Monguzzi, A.; Bianchi, F.; Bianchi, A.; Mauri, M.; Simonutti, R.; Ruffo, R.; Tubino, R.; Meinardi, F. *Adv. Ener. Mater.* **2013**, *3*, 680.
(23) Marsico, F.; Turshatov, A.; Peköz, R.; Avlasevich, Y.; Wagner, M.; Weber, K.; Donadio, D.; Landfester, K.; Baluschev, S.; Wurm, F. R. *J. Am. Chem. Soc.* **2014**, *136*, 11057.
(24) Hauptvogel, I. M.; Biedermann, R.; Klein, N.; Senkovska, I.; Cadiau, A.; Wallacher, D.; Feyerherm, R.; Kaskel, S. *Inorg. Chem.* **2011**, *50*, 8367.
(25) Kent, C. A.; Mehl, B. P.; Ma, L. Q.; Papanikolas, J. M.; Meyer, T. J.; Lin, W. B. *J. Am. Chem. Soc.* **2010**, *132*, 12767.
(26) Zhang, T.; Lin, W. *Chem. Soc. Rev.* **2014**, *43*, 5982.
(27) Liu, J. X.; Zhou, W. C.; Liu, J. X.; Howard, I.; Kilibarda, G.; Schlabach, S.; Coupry, D.; Addicoat, M.; Yoneda, S.; Tsutsui, Y.; Sakurai, T.; Seki, S.; Wang, Z. B.; Lindemann, P.; Redel, E.; Heine, T.; Wöll, C. *Angew. Chem., Int. Ed.* **2015**, *54*, 7441.
(28) Alkordi, M. H.; Liu, Y.; Larsen, R. W.; Eubank, J. F.; Eddaoudi, M. *J. Am. Chem. Soc.* **2008**, *130*, 12639.
(29) Juan-Alcañiz, J.; Gascon, J.; Kapteijn, F. *J. Mater. Chem.* **2012**, *22*, 10102.
(30) Pope, M.; Swenberg, C. E. *Electronic Processes in Organic Crystals and Polymers*; Oxford University Press: New York, 1999.
(31) Wohnhaas, C.; Friedemann, K.; Busko, D.; Landfester, K.; Baluschev, S.; Crespy, D.; Turshatov, A. *ACS Macro Lett.* **2013**, *2*, 446.
(32) Svagan, A. J.; Busko, D.; Avlasevich, Y.; Glasser, G.; Baluschev, S.; Landfester, K. *ACS Nano* **2014**, *8*, 8198.
(33) Miller, K. S.; Krochta, J. M. *Trends Food Sci. Technol.* **1997**, *8*, 228.
(34) Maeda, Y.; Paul, D. R. *J. Polym. Sci., Part B: Polym. Phys.* **1987**, *25*, 1005.
(35) Furukawa, S.; Reboul, J.; Diring, S.; Sumida, K.; Kitagawa, S. *Chem. Soc. Rev.* **2014**, *43*, 5700.
(36) Sindoro, M.; Yanai, N.; Jee, A. Y.; Granick, S. *Acc. Chem. Res.* **2014**, *47*, 459.
(37) Cheng, Y. Y.; Fuckel, B.; Khoury, T.; Clady, R. G. C. R.; Tayebjee, M. J. Y.; Ekins-Daukes, N. J.; Crossley, M. J.; Schmidt, T. W. *J. Phys. Chem. Lett.* **2010**, *1*, 1795.
(38) Turro, N. J.; Ramamurthy, V.; Scaiano, J. C. *Modern Molecular Photochemistry of Organic Molecules*; University Science Books: Sausalito, CA, 2010.
(39) Monguzzi, A.; Mezyk, J.; Scotognella, F.; Tubino, R.; Meinardi, F. *Phys. Rev. B: Condens. Matter Mater. Phys.* **2008**, *78*, 195112.
(40) Haefele, A.; Blumhoff, J.; Khnayzer, R. S.; Castellano, F. N. *J. Phys. Chem. Lett.* **2012**, *3*, 299.
(41) Gray, V.; Dzebo, D.; Abrahamsson, M.; Albinsson, B.; Moth-Poulsen, K. *Phys. Chem. Chem. Phys.* **2014**, *16*, 10345.
(42) Schmidt, T. W.; Castellano, F. N. *J. Phys. Chem. Lett.* **2014**, *5*, 4062.
(43) Gadzikwa, T.; Lu, G.; Stern, C. L.; Wilson, S. R.; Hupp, J. T.; Nguyen, S. T. *Chem. Commun.* **2008**, 5493.
(44) Gadzikwa, T.; Farha, O. K.; Malliakas, C. D.; Kanatzidis, M. G.; Hupp, J. T.; Nguyen, S. T. *J. Am. Chem. Soc.* **2009**, *131*, 13613.
(45) Kondo, M.; Furukawa, S.; Hirai, K.; Kitagawa, S. *Angew. Chem., Int. Ed.* **2010**, *49*, 5327.
(46) Liu, B.; Ma, M. Y.; Zacher, D.; Bétard, A.; Yusenko, K.; Metzler-Nolte, N.; Wöll, C.; Fischer, R. A. *J. Am. Chem. Soc.* **2011**, *133*, 1734.
(47) Yanai, N.; Granick, S. *Angew. Chem., Int. Ed.* **2012**, *51*, 5638.
(48) Nagata, S.; Sato, H.; Sugikawa, K.; Kokado, K.; Sada, K. *CrystEngComm* **2012**, *14*, 4137.
(49) Morris, W.; Briley, W. E.; Auyeung, E.; Cabezas, M. D.; Mirkin, C. A. *J. Am. Chem. Soc.* **2014**, *136*, 7261.
(50) So, M. C.; Wiederrecht, G. P.; Mondloch, J. E.; Hupp, J. T.; Farha, O. K. *Chem. Commun.* **2015**, *51*, 3501.
(51) Yoshihara, T.; Yamaguchi, Y.; Hosaka, M.; Takeuchi, T.; Tobita, S. *Angew. Chem., Int. Ed.* **2012**, *51*, 4148.
(52) Khnayzer, R. S.; Blumhoff, J.; Harrington, J. A.; Haefele, A.; Deng, F.; Castellano, F. N. *Chem. Commun.* **2012**, *48*, 209.
(53) Yanai, N.; Kimizuka, N. *Chem. Commun.* **2016**, *52*, 5354.

DOI: 10.1021/jacs.6b01652
J. Am. Chem. Soc. 2016, 138, 6541−6549